

UCLA

UCLA Previously Published Works

Title

Analysis of island dynamics in epitaxial growth of thin films

Permalink

<https://escholarship.org/uc/item/8v07g7xj>

Journal

Multiscale Modeling & Simulation, 1(1)

ISSN

1540-3459

Authors

Caflisch, Russel E

Li, B

Publication Date

2003

Peer reviewed

ANALYSIS OF ISLAND DYNAMICS IN EPITAXIAL GROWTH OF THIN FILMS*

RUSSEL E. CAFLISCH[†] AND BO LI[‡]

Abstract. This work is concerned with analysis and refinement for a class of island dynamics models for epitaxial growth of crystalline thin films. An island dynamics model consists of evolution equations for step edges (or island boundaries), coupled with a diffusion equation for the adatom density, on an epitaxial surface. The island dynamics model with irreversible aggregation is confirmed to be mathematically ill-posed, with a growth rate that is approximately linear for large wavenumbers. By including a kinetic model for the structure and evolution of step edges, the island dynamics model is made mathematically well-posed. In the limit of small edge Péclet number, the edge kinetics model reduces to a set of boundary conditions, involving line tension and one-dimensional surface diffusion, for the adatom density. Finally, in the infinitely fast terrace diffusion limit, a simplified model of one-dimensional surface diffusion and kink convection is derived and found to be linearly stable.

Key words. epitaxial growth, island dynamics, step edges, normal velocity, adatom diffusion, linear stability, step-edge kinetics, line tension, surface diffusion

AMS subject classifications. 35Q99, 35R35

PII. S1540345902407208

1. Introduction. Epitaxy is the growth of a thin film on a substrate in which the crystal properties of the film are inherited from those of the substrate. Since an epitaxial film can (at least in principle) grow as a single crystal without grain boundaries or other defects, this method produces crystals of the highest quality. In spite of its ideal properties, epitaxial growth is still challenging to mathematically model and numerically simulate because of the wide range of length and time scales that it encompasses, from the atomistic to the continuum.

Burton, Cabrera, and Frank [2] developed the first detailed theoretical description for epitaxial growth. In this “BCF” model, the adatom density solves a diffusion equation with an equilibrium boundary condition ($\rho = \rho_{eq}$), and step edges (or island boundaries) move at a velocity determined from the diffusive flux to the boundary. Modifications of this theory were made, for example, in [8, 9, 12, 13] to include additional effects such as curvature of the boundary, but these are all for near equilibrium. Numerical simulation of island dynamics, using a level set method, was implemented in [4, 5, 10, 14]. A fully nonequilibrium modeling approach was formulated in [3] using an atomistic, kinetic model for the structure and the evolution of a step edge (island boundary). These are “island dynamics” models, since they describe an epitaxial surface by the location and evolution of the island boundaries and step edges. They employ coarse graining in the lateral directions, but they retain atomistic discreteness in the growth direction.

The present article is concerned with the analysis and refinement of island dy-

*Received by the editors May 7, 2002; accepted for publication (in revised form) October 7, 2002; published electronically January 28, 2003. This research was supported in part by NSF and DARPA through grant NSF-DMS 9615854 as part of the Virtual Integrated Prototyping Initiative, by ARO through grant DAAG98-1-0323, by NSF through grant DMS-0072958, and by a Focused Research Group grant DMS-0074152 from the NSF.

<http://www.siam.org/journals/mms/1-1/40720.html>

[†]Department of Mathematics and California NanoSystem Institute, University of California, 405 Hilgard Avenue, Los Angeles, CA 90095-1555 (caflisch@math.ucla.edu).

[‡]Department of Mathematics, University of Maryland, College Park, MD 20742-4015 (bli@math.umd.edu).

namics models. The models are developed here in the context of step-flow growth for an epitaxial surface consisting of a periodic step train, and their stability and asymptotic properties are analyzed.

Several assumptions are employed in this analysis to simplify the results and reduce the number of parameters: Asymmetric step-edge attachment due to the Ehrlich–Schwoebel barrier is not included, partly because it is believed to be absent from many semiconductor systems. The hopping rate to a step from a terrace is set equal to the hopping rate along the terrace, and the hopping rate from a step to a terrace is set equal to the hopping rate along the step. The assumptions on the hopping rates correspond to the rates in an “ E_S - E_N ” KMC model [6]. The epitaxial surface is assumed to consist of an infinite train of parallel steps, with orientation close to a crystallographic direction. Finite lattice spacing corrections are omitted from these models, since their effect on the results here is small. The lattice size correction and equality of hopping rates on a terrace and to a step would imply that the kinetic coefficient in the adatom boundary condition is infinite (see [18, Chapter 10], and [20]); i.e., the diffusive flux term $D\mathbf{n} \cdot \nabla\rho$ would be absent in the boundary conditions on ρ . Nevertheless, this correction would not significantly change the results of our analysis. Desorption and nucleation are omitted from this analysis, since their effect is small for many systems. Any of these restrictions are easily removed to generalize the results of this analysis.

The first and simplest island dynamics model involves *irreversible aggregation*. The corresponding boundary condition is that the adatom density vanishes on island boundaries or step edges. This follows from the assumption that an adatom sticks irreversibly to a boundary immediately after it hits the boundary. This model is mathematically equivalent to the BCF model, since $\rho^{BCF} - \rho_{eq}$ satisfies the equations of this model.

As expected, we find that the island dynamics model with irreversible aggregation is mathematically ill-posed and that a Mullins–Sekerka-type dendritic instability occurs in the motion of step edges for large wavenumbers [15, 16]. The instability is weak, since the growth rate in the dispersion relation is asymptotically linear as a function of wavenumber, and it has a small coefficient due to two-sided attachment.

The next model is the island dynamics model with *edge kinetics*. It involves not only the island boundaries and the adatom density but also the density of edge-atoms—atoms that diffuse along island boundaries—and the density of kinks along island boundaries. Both the attachment and detachment of adatoms to and from the boundaries are included in the model. The underlying equations include a diffusion equation for the adatom density together with a mixed-type boundary condition, a diffusion equation for the edge-atom density, and a convection equation for the kink density.

For the linear stability analysis of the island dynamics model with edge kinetics, we consider only the steady and quasi-steady systems. This is justified by the large magnitude of terrace adatom diffusion constant D_T for most practical applications. In the range of realistic parameters, both systems are linearly stable, with decay rate proportional to l^2 , for both small and large wavenumbers l . The constants of proportionality are solely characterized by the “edge Péclet number” P_E , an input parameter that is proportional to both the constant deposition flux rate and the step width but inversely proportional to the edge diffusion constant D_E . In fact, for small edge Péclet numbers, both systems are stable for all wavenumbers. Note that the Bales–Zangwill-type instability of a step edge [1] is not present due to the exclusion of asymmetry in boundary attachment and the inclusion of edge-atom diffusion and

kink convection in the model.

The edge kinetics model can be directly solved in the limit of small edge Péclet number to yield new formulas for the normal velocity and for the boundary conditions on the adatom density. These include line tension and one-dimensional surface diffusion (i.e., surface diffusion along the step edge) terms of the usual Gibbs–Thomson type, but with parameters that come from a kinetic steady state rather than from a thermodynamic driving force. To our knowledge, this is the first derivation of line tension and surface diffusion from a kinetic, atomistic approach. Stability analysis for the resulting system is contained in [8, 12, 13].

Alternatively, in the infinitely fast terrace diffusion limit, the island dynamics model with edge kinetics reduces to a simplified model that involves only the edge-atom density and kink density on a step edge (but not the adatom density on the terraces). We find that the dispersion relation for the original island dynamics model with edge kinetics is qualitatively recaptured by this simplified model.

Most related works on island dynamics models start from a coarse-grained or thermodynamic description, as opposed to the atomistic description that is the basis for our analysis. For example, Pierre-Louis [17] formulates a model that is similar to our island dynamics model with edge kinetics, but his model comes from a free energy that already contains the Gibbs–Thomson term. Similarly, the derivation of surface diffusion outlined in [11] includes a Gibbs–Thomson term in the adatom boundary condition and is similar to our approach. The review article of [19] describes different forms of the diffusion coefficient that are appropriate for a coarse-grained description of rough growth in various regimes.

In section 2, the general framework of the island dynamics models is formulated. Section 3 contains the linear stability analysis for the island dynamics model with irreversible aggregation. In section 4, the island dynamics model with edge kinetics and its linear stability are described. Section 5 describes the limit of small edge Péclet number, including boundary conditions and normal velocity that involve line tension and surface diffusion terms. In section 6, a simplified model of surface diffusion and kink convection is derived under the assumption of the infinitely fast terrace diffusion, and its linear stability is analyzed. In section 7, conclusions of our analysis and comparison of the different models are presented. Finally, various details are gathered in four appendices.

2. Island dynamics models. This section provides a general formulation of an island dynamics model applied to step-flow growth of an epitaxial thin film.

Consider a simple cubic crystal with lattice spacing a and with crystallographic directions parallel to the x , y , and z axes. For notational convenience, nondimensionalize spatial coordinates (x, y, z) , diffusion coefficient D , number density per area ρ , and number density per length ϕ as

$$\begin{aligned} (2.1) \quad & (x, y, z) \rightarrow (x/a, y/a, z/a) && \text{spatial coordinate,} \\ (2.2) \quad & D \rightarrow D/a^2 && \text{diffusion coefficient,} \\ (2.3) \quad & \rho \rightarrow a^2\rho && \text{two-dimensional density,} \\ (2.4) \quad & \phi \rightarrow a\phi && \text{one-dimensional density.} \end{aligned}$$

This is equivalent to measuring all distances in units of a or to setting $a = 1$.

Assume that the crystal surface consists of a periodic sequence of step edges that are approximately straight and parallel to the y -axis, as in Figure 2.1. Each step is one atomic layer lower than the preceding one to its left, and the steps move to the

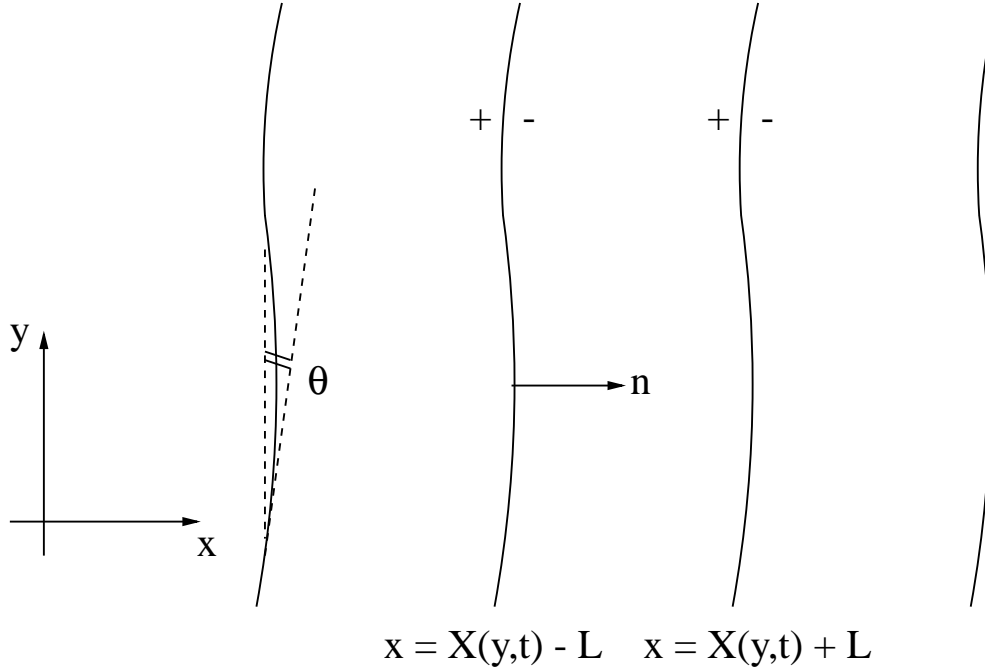


FIG. 2.1. The geometry of periodic step-flow growth of a crystal.

right during crystal growth. These step edges are represented as

$$x = X(y, t) + (2j + 1)L, \quad j = 0, \pm 1, \dots,$$

in which $X(y, t)$ is a smooth function and $L > 0$ is half of the step width. For each point $(X(y, t), y)$ on a step edge, let $\theta = \theta(y, t)$ denote the signed angle between the tangent of the step edge and the y -axis; i.e.,

$$(2.5) \quad \tan \theta = -\partial_y X, \quad -\pi/2 < \theta < \pi/2.$$

The curvature $\kappa = \kappa(y, t)$, the unit normal $\mathbf{n} = \mathbf{n}(y, t)$ pointing from the upper terrace into lower terrace, and the normal velocity $v = v(y, t)$ of the step edge are given by

$$(2.6) \quad \kappa = \partial_s \theta, \quad \mathbf{n} = (\cos \theta, \sin \theta), \quad v = (\partial_t X) \cos \theta,$$

in which ∂_s is the tangential derivative in the y -direction. Note that the sign of θ has been changed from that used in [3] to avoid a minus sign in the definition of curvature κ . From (2.5) and (2.6), the formulas for \mathbf{n} and v are

$$(2.7) \quad \mathbf{n} = \frac{1}{\sqrt{1 + (\partial_y X)^2}} (1, -\partial_y X) \quad \text{and} \quad v = \frac{\partial_t X}{\sqrt{1 + (\partial_y X)^2}}.$$

Epitaxial growth involves deposition, diffusion, and attachment of adatoms on the surface. Deposition is from an external source, such as a molecular beam. The adatoms on the surface can be described by an adatom density function $\rho = \rho(x, y, t)$, which is assumed to be periodic in x with period $2L$. Adatom diffusion on the epitaxial surface is described by a diffusion equation of the form

$$(2.8) \quad \partial_t \rho - D_T \nabla^2 \rho = F \quad \text{for } X(y, t) - L < x < X(y, t) + L,$$

in which D_T and F are the terrace diffusion constant and the deposition flux rate, respectively, after spatial nondimensionalization as in (2.1)–(2.4). For simplicity, we have left out desorption and nucleation terms on the right-hand side of (2.8). Attachment of adatoms to the step edges and the resulting motion of the step edges are described by boundary conditions at the step edges for the diffusion equation and a formula for the step-edge velocity v .

Denote the restriction of any function w to the step edge from upper and lower terraces as w_+ and w_- , respectively, as indicated in Figure 2.1. The net flux to the step edge from upper and lower terraces is denoted as $f_+ = f_+(y, t)$ and $f_- = f_-(y, t)$, respectively, in which

$$(2.9) \quad v\rho_+ + D_T \mathbf{n} \cdot \nabla \rho_+ = -f_+ \quad \text{at } x = X(y, t) + L,$$

$$(2.10) \quad v\rho_- + D_T \mathbf{n} \cdot \nabla \rho_- = f_- \quad \text{at } x = X(y, t) - L.$$

The total flux is $f = f_+ + f_-$ given by

$$f = -v[\rho] - D_T[\mathbf{n} \cdot \nabla \rho],$$

in which the square bracket $[\]$ is defined as the difference across the step; i.e., for any w

$$[w] = w_+ - w_-.$$

The principal dimensionless parameters for epitaxial growth are the ratios of flux and diffusive coefficients, which we refer to as “Péclet numbers” by analogy with fluid mechanics. In steady state the flux to an edge and the edge velocity are $f_0 = 2FL$ and $v_0 = f_0$. Let P_T be the terrace Péclet number and P_E be the edge Péclet number, defined as

$$(2.11) \quad P_T = v_0/D_T = 2FL/D_T,$$

$$(2.12) \quad P_E = 2FL/D_E,$$

in which D_E is the edge diffusion constant. An additional frequently used dimensionless parameter is

$$R = F/D_T = P_T/2L.$$

Different island dynamics models are distinguished by having different diffusive boundary conditions and different normal velocity. The following is a summary of the four island dynamics models that are analyzed in this paper, of which the fourth does not involve an adatom density:

1. *The island dynamics model with irreversible aggregation (section 3):*

$$\begin{aligned} \rho &= 0 & \text{at } x = X(y, t) \pm L, \\ v &= f. \end{aligned}$$

2. *The island dynamics model with step-edge kinetics (section 4):*

$$\begin{aligned} f_+ &= D_T \rho_+ - D_E \phi & \text{at } x = X(y, t) + L, \\ f_- &= D_T \rho_- - D_E \phi & \text{at } x = X(y, t) - L, \\ v &= k w \cos \theta, \end{aligned}$$

in which f_{\pm} are defined by (2.9) and (2.10), D_E is the (spatially nondimensionalized) diffusion coefficient for both edge diffusion and edge detachment, ϕ and k are the densities of edge-atoms and kinks, and w is the kink velocity, defined in section 4. The velocity law given in the last equation above was first derived in Appendix A of [9].

3. *The island dynamics model with line tension and surface diffusion (section 5):*

$$\begin{aligned} f_+ &= D_T(\rho_+ - \rho_*) - \mu\kappa && \text{at } x = X(y, t) + L, \\ f_- &= D_T(\rho_- - \rho_*) - \mu\kappa && \text{at } x = X(y, t) - L, \\ v &= D_T \mathbf{n} \cdot [\nabla \rho] + \beta \rho_{*yy} + (\mu/D_E) \kappa_{yy}, \end{aligned}$$

in which κ is curvature and ρ_* , β , and μ are defined in section 5.

4. *The infinitely fast terrace diffusion limit (section 6):*

$$v = l_1 D_E \phi k \cos \theta,$$

in which l_1 is a constant defined in section 6.

3. Island dynamics with irreversible aggregation. The island dynamics model with irreversible aggregation for the periodic step-train problem consists of the following diffusion equation, boundary conditions, and velocity law:

$$(3.1) \quad \partial_t \rho - D_T \nabla^2 \rho = F \quad \text{for } X(y, t) - L < x < X(y, t) + L,$$

$$(3.2) \quad \rho = 0 \quad \text{at } x = X(y, t) \pm L,$$

$$(3.3) \quad v = -D_T \mathbf{n} \cdot [\nabla \rho],$$

in which the adatom density $\rho = \rho(x, y, t)$ is assumed to be periodic in x with period $2L$, and v is the normal velocity defined in (2.6). For simplicity, the term $v[\rho]$ in the flux f is omitted, since it is small for large values of D_T/F that typically occur in molecular beam epitaxy (MBE).

A steady planar solution of (3.1)–(3.3) is given by

$$(3.4) \quad X_0(y, t) = v_0 t,$$

$$(3.5) \quad v_0 = 2FL,$$

$$(3.6) \quad \rho_0 = b_0 + b_1 \tilde{x} + b_2 e^{-P_T \tilde{x}},$$

$$(3.7) \quad \tilde{x} = x - v_0 t,$$

in which

$$b_0 = (1/2) \coth(P_T L), \quad b_1 = -(2L)^{-1}, \quad b_2 = -(2 \sinh(P_T L))^{-1}.$$

Next we perform linear analysis for perturbations of this planar solution. Set

$$X = X_0 + \varepsilon X_1, \quad \rho = \rho_0 + \varepsilon \rho_1, \quad \mathbf{n} = \mathbf{n}_0 + \varepsilon \mathbf{n}_1, \quad v = v_0 + \varepsilon v_1,$$

where ε is a parameter small in magnitude. By (2.7), the unit normal is $\mathbf{n}_1 = (0, -\partial_y X_1)$ and the normal velocity is $v_1 = \partial_t X_1$. The linearized equations for $\rho_1 = \rho_1(\tilde{x}, y, t)$ are

$$(3.8) \quad \partial_t \rho_1 - v_0 \partial_{\tilde{x}} \rho_1 - D_T \nabla^2 \rho_1 = 0 \quad \text{for } -L < \tilde{x} < L,$$

$$(3.9) \quad \rho_1 + X_1 \rho_0' = 0 \quad \text{at } \tilde{x} = \pm L,$$

$$(3.10) \quad \partial_t X_1 = -D_T [\partial_{\tilde{x}} \rho_1] - D_T X_1 [\rho_0''],$$

where the jumps are defined using the limiting values at $\pm L$. These equations are derived using perturbation theory for a free boundary, as described in Appendix A.

Principal mode solutions (X_1, ρ_1) have the form

$$X_1 = \hat{X}_1 e^{\omega t + i l y} \quad \text{and} \quad \rho_1 = \left(\hat{\rho}_+ e^{\hat{D}_{T+} \hat{x}} + \hat{\rho}_- e^{\hat{D}_{T-} \hat{x}} \right) e^{\omega t + i l y},$$

where l is the wavenumber and \hat{X} , $\hat{\rho}_+$, $\hat{\rho}_-$, \hat{D}_{T+} , \hat{D}_{T-} , and ω are all constants. For these solutions, (3.9) and (3.10) are equivalent to

$$\begin{aligned} \hat{\rho}_+ e^{\hat{D}_{T+} L} + \hat{\rho}_- e^{\hat{D}_{T-} L} + \hat{X}_1 \rho'_0(L) &= 0, \\ \hat{\rho}_+ e^{-\hat{D}_{T+} L} + \hat{\rho}_- e^{-\hat{D}_{T-} L} + \hat{X}_1 \rho'_0(-L) &= 0, \\ \omega \hat{X}_1 &= -2D_T \left(\hat{D}_{T+} \hat{\rho}_+ \sinh(\hat{D}_{T+} L) + \hat{D}_{T-} \hat{\rho}_- \sinh(\hat{D}_{T-} L) \right) - D_T \hat{X}_1 (\rho''_0(L) - \rho''_0(-L)), \end{aligned}$$

which imply

$$\begin{vmatrix} e^{\hat{D}_{T+} L} & e^{\hat{D}_{T-} L} & \rho'_0(L) \\ e^{-\hat{D}_{T+} L} & e^{-\hat{D}_{T-} L} & \rho'_0(-L) \\ -2D_T \hat{D}_{T+} \sinh(\hat{D}_{T+} L) & -2D_T \hat{D}_{T-} \sinh(\hat{D}_{T-} L) & -D_T (\rho''_0(L) - \rho''_0(-L)) + \omega \end{vmatrix} = 0.$$

This is equivalent to

$$\begin{aligned} (3.11) \quad & \left\{ \coth(\hat{D}_{T+} L) - \coth(\hat{D}_{T-} L) \right\} \left\{ D_T (\rho''_0(L) - \rho''_0(-L)) + \omega \right\} \\ & + D_T \left(\hat{D}_{T-} - \hat{D}_{T+} \right) \cdot (\rho'_0(L) + \rho'_0(-L)) \\ & + D_T (\rho'_0(L) - \rho'_0(-L)) \left\{ \hat{D}_{T+} \coth(\hat{D}_{T-} L) - \hat{D}_{T-} \coth(\hat{D}_{T+} L) \right\} = 0. \end{aligned}$$

Similarly, insertion of ρ_1 into (3.8) leads to

$$(3.12) \quad D_T \hat{D}_{T+}^2 + v_0 \hat{D}_{T+} - (\omega + D_T l^2) = 0,$$

$$(3.13) \quad D_T \hat{D}_{T-}^2 + v_0 \hat{D}_{T-} - (\omega + D_T l^2) = 0.$$

Equations (3.11)–(3.13) determine $\hat{D}_{T+} = \hat{D}_{T+}(l)$, $\hat{D}_{T-} = \hat{D}_{T-}(l)$, and the growth rate $\omega = \omega(l)$.

PROPOSITION 3.1. *For the island dynamics with irreversible aggregation, the growth rate $\omega = \omega(l)$ satisfies*

$$(3.14) \quad \omega = \omega_0 l + o(l) \quad \text{as } l \rightarrow \infty,$$

where

$$\omega_0 = D_T (\rho'_0(L) + \rho'_0(-L)) > 0.$$

Proof. Observe from (3.11) that $\omega = \omega(l)$ is of order not greater than $O(\hat{D}_{T\pm}(l))$. However, by (3.12) and (3.13), \hat{D}_{T+} and \hat{D}_{T-} are the two roots of the same quadratic equation. Hence,

$$\hat{D}_{T+} + \hat{D}_{T-} = -\frac{v_0}{D_T} \quad \text{and} \quad \hat{D}_{T+} \hat{D}_{T-} = -\frac{\omega + D_T l^2}{D_T}.$$

Consequently, both \hat{D}_{T+} and \hat{D}_{T-} have the leading order terms l and $-l$, respectively. By examining the leading order term in (3.11), we obtain the desired asymptotic expansion (3.14) by a series of calculations. Finally, a direct verification using (3.4), (3.5), and (2.11) leads to

$$\rho'_0(L) + \rho'_0(-L) = \frac{P_T L \cosh(P_T L) - \sinh(P_T L)}{L \sinh(P_T L)} > 0.$$

The proof is complete. \square

Our analysis shows that the irreversible aggregation model of island dynamics is mathematically ill-posed. However, the instability of the step-edge motion predicted by the model is weak, since the growth rate ω depends on the wavenumber l linearly up to the leading order, and since the coefficient, ω_0 , of the leading order term can be shown to be $v_0 (P_T L v_0 / 3 + O((P_T L)^3))$ in the small terrace Péclet number asymptotic expansion. In fact, for the quasi-steady system—the system obtained by dropping the term $\partial_t \rho$ in (3.1)–(3.3)—one can show easily that the growth rate is $\omega = 0$. In section 5, we propose more physically acceptable boundary conditions derived from the step-edge kinetics to replace the irreversibility condition in this model.

4. Island dynamics with the kinetic edge model.

4.1. The kinetic edge model. The kinetic edge model of island dynamics was first developed in [3]. It involves a statistical description of the crystalline structure of a step edge, including the edge-atom density $\phi = \phi(y, t)$ and the kink density $k = k(y, t)$. Edge-atoms are atoms with a single in-plane neighbor along the step; kinks are atoms with two in-plane neighbors. Kinks are of two types—right-facing kinks and left-facing kinks—the densities of which are denoted by k_r and k_ℓ . The total kink density and the relation between the kink density and the normal angle are

$$(4.1) \quad k_r + k_\ell = k,$$

$$(4.2) \quad k_r - k_\ell = \tan \theta,$$

as determined by [2].

The kinetic edge model consists of a diffusion equation for the edge-atom density ϕ and a convection equation for the kink density k

$$(4.3) \quad \partial_t \phi - D_E \partial_s^2 \phi = f_+ + f_- - f_0,$$

$$(4.4) \quad \partial_t k + \partial_s(w(k_r - k_\ell)) = 2(g - h).$$

In (4.3), D_E is the edge diffusion coefficient, f_\pm are the net fluxes to the edge from terraces as defined in (2.9) and (2.10), and f_0 is the net loss term due to the attachment of edge-atoms to kinks. In (4.4), w is the kink velocity, and g and h represent, respectively, the creation and annihilation of left-right kink pairs. Note that left-facing kinks and right-facing kinks move in opposite directions with velocity w and $-w$, respectively.

The quantities f_+ , f_- , f_0 , w , g , h , and v are determined by the following consti-

tutive relations:

$$(4.5) \quad f_+ = D_T \rho_+ - D_E \phi,$$

$$(4.6) \quad f_- = D_T \rho_- - D_E \phi,$$

$$(4.7) \quad f_0 = v(\phi \kappa + 1) = v(1 - \phi X_{yy}),$$

$$(4.8) \quad w = l_1 D_E \phi + D_T(l_2 \rho_+ + l_3 \rho_-) = l_{123} D_E \phi + l_2 f_+ + l_3 f_-,$$

$$(4.9) \quad g = \phi(m_1 D_E \phi + D_T(m_2 \rho_+ + m_3 \rho_-)) = \phi(m_{123} D_E \phi + m_2 f_+ + m_3 f_-),$$

$$(4.10) \quad h = k_r k_\ell (n_1 D_E \phi + D_T(n_2 \rho_+ + n_3 \rho_-)) = k_r k_\ell (n_{123} D_E \phi + n_2 f_+ + n_3 f_-),$$

$$(4.11) \quad X_t = v = w k \cos \theta,$$

where D_T is the (diffusion) hopping rate of an adatom on a terrace, D_E is the (diffusion) hopping rate of an edge-atom along or off an edge, and all l_i, m_i, n_i ($i = 1, 2, 3$) are nonnegative numbers. The geometric parameters l_i, m_i, n_i count the number of paths from one state to another; cf. [3] for details. Here, these parameters are generalized to include a factor relating the macroscopic density ρ or ϕ to the local density of adatoms or edge atoms at a specific site. For convenience, we have used the notation

$$q_{ij} = q_i + q_j \quad \text{and} \quad q_{ijk} = q_i + q_j + q_k$$

for $q = l, m$, or n . The constitutive laws (4.5)–(4.10) have been simplified by omission of terms that are insignificant for the kinetic steady-state solutions of relevance to step-flow growth. The neglected terms are physically important, however, since they are necessary for detailed balance and for equilibrium solutions; they are included in the more complete analysis of [3].

The relations (4.5), (4.6), and (4.8)–(4.10) are determined by a mean field theory [3]. Equation (4.7) is derived from the conservation of mass [3], and (4.11) comes from counting adatoms as part of the crystal once they have attached to a kink; cf. Appendix A in [9]. Note that for simplicity a number of physical effects have been neglected. They include the desorption of adatoms into vapor, the nucleation of islands on steps, and the Ehrlich–Schwoebel effect [7, 21, 22]. In [3] the parameters l_i, m_i , and n_i are fixed to be $(l_1, l_2, l_3) = (2, 2, 1)$, $(m_1, m_2, m_3) = (2, 4, 2)$, and $(n_1, n_2, n_3) = (2, 3, 1)$, which follow from a simple geometric counting argument, but in the present work they are allowed to be arbitrary parameters.

4.2. Quasi-steady island dynamics with the kinetic edge model. For simplicity in the subsequent analysis, consider the “quasi-steady” island dynamics model consisting of the kinetic edge model (4.1)–(4.11), combined with quasi-steady adatom diffusion equation

$$(4.12) \quad -D_T \nabla^2 \rho = F \quad \text{for } X(y, t) - L < x < X(y, t) + L,$$

$$(4.13) \quad D_T \mathbf{n} \cdot \nabla \rho_+ = -f_+ \quad \text{at } x = X(y, t) + L,$$

$$(4.14) \quad D_T \mathbf{n} \cdot \nabla \rho_- = f_- \quad \text{at } x = X(y, t) - L.$$

We also consider the “steady” island dynamics model that is obtained by replacing (4.3) and (4.4) in the quasi-steady system by

$$(4.15) \quad -D_E \partial_s^2 \phi = f_+ + f_- - f_0,$$

$$(4.16) \quad \partial_s(w(k_r - k_\ell)) = 2(g - h).$$

In the steady system, dynamics is retained only in the equation for the step-edge position X .

4.3. Planar steady-state solution. Let $X_0(y, t) = v_0 t$ define the step-edge position, where $v_0 > 0$ is a constant. The corresponding angle, curvature, and normal are $\theta_0 = 0$, $\kappa_0 = 0$, and $\mathbf{n}_0 = (0, 1)$, respectively. Assuming that the adatom density ρ_0 is independent of y and that both the edge-atom density ϕ_0 and the kink density k_0 are constants, we obtain then from (4.3)–(4.14) the following steady-state solution:

$$(4.17) \quad X_0(y, t) = v_0 t,$$

$$(4.18) \quad v_0 = 2FL,$$

$$(4.19) \quad \rho_0(x, t) = -\frac{F}{2D_T} ((x - v_0 t)^2 - L^2) + \frac{D_E \phi_0 + FL}{D_T}$$

for $|x - v_0 t| < L$,

$$(4.20) \quad f_{00} = 2f_{+0} = 2f_{-0} = 2FL,$$

$$(4.21) \quad k_0 = \frac{2FL}{w_0},$$

$$(4.22) \quad w_0 = l_{123} D_E \phi_0 + l_{23} FL,$$

$$(4.23) \quad g_0 = \phi_0 (m_{123} D_E \phi_0 + m_{23} FL),$$

$$(4.24) \quad h_0 = \frac{1}{4} k_0^2 (n_{123} D_E \phi_0 + n_{23} FL),$$

$$(4.25) \quad g_0 = h_0.$$

Note that the last equation determines ϕ_0 .

In [3], the solution of these equations was found to scale with ε defined as

$$(4.26) \quad \varepsilon = P_E^{1/3}$$

in which P_E is the edge Péclet number defined in (2.12). This is described more precisely in the following proposition, the proof of which is presented in Appendix B.

PROPOSITION 4.1. *Suppose $l_{123} \neq 0$ and $m_{123} \neq 0$. Then*

$$(4.27) \quad \phi_0 = \left(\frac{n_{123}}{4l_{123}^2 m_{123}} \right)^{1/3} \varepsilon^2 + O(\varepsilon^3) \quad \text{as } \varepsilon \rightarrow 0,$$

$$(4.28) \quad k_0 = \left(\frac{l_{123} n_{123}}{4m_{123}} \right)^{1/3} \varepsilon + O(\varepsilon^2) \quad \text{as } \varepsilon \rightarrow 0.$$

Suppose $l_{23} \neq 0$, $m_{23} \neq 0$, and $n_{23} \neq 0$. Let

$$(4.29) \quad \sigma_0 = \frac{n_{23}}{l_{23}^2 m_{23}} \quad \text{and} \quad \sigma_1 = 2\sigma_0^2 \left(\frac{n_1}{n_{23}} - \frac{m_1}{m_{23}} - \frac{2l_1}{l_{23}} - 2 \right).$$

Then

$$(4.30) \quad \phi_0 \rightarrow \sigma_0 \quad \text{and} \quad k_0 \rightarrow 2/l_{23} \quad \text{as } \varepsilon \rightarrow \infty.$$

Moreover, if $\sigma_1 < 0$, then ϕ_0 is a strictly increasing function of ε in $(0, \infty)$; if $\sigma_1 > 0$, then there exists a value $\varepsilon_0 > 0$ such that ϕ_0 is a strictly increasing function of ε for $0 < \varepsilon < \varepsilon_0$.

We remark that the case where $l_{23} = m_{23} = n_{23} = 0$ is included in our simplified model in section 6 below; cf. (6.4). In Figure 4.1, we plot the graph of ϕ_0 and k_0 as functions of $\varepsilon = P_E^{1/3}$ with $(l_1, l_2, l_3) = (2, 2, 1)$, $(m_1, m_2, m_3) = (2, 4, 2)$, and $(n_1, n_2, n_3) = (2, 3, 1)$, which are the parameters used in [3] and satisfy $\sigma_1 < 0$.

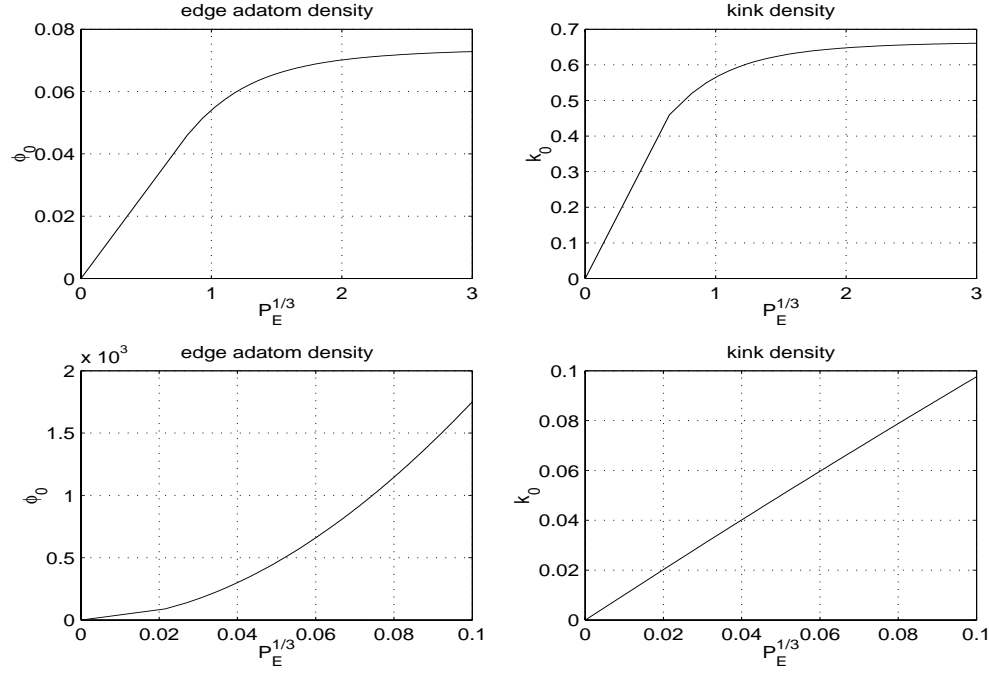


FIG. 4.1. The steady-state edge-atom density and kink density as functions of $\varepsilon = P_E^{1/3}$ with $(l_1, l_2, l_3) = (2, 2, 1)$, $(m_1, m_2, m_3) = (2, 4, 2)$, and $(n_1, n_2, n_3) = (2, 3, 1)$. The corresponding top and bottom plots differ only by scales.

4.4. Linear stability analysis for island dynamics with the kinetic edge model. Consider a perturbation around the steady planar solution, defined as

$$\begin{aligned} & (X, \rho, \phi, k, \theta, \kappa, \mathbf{n}, v, f_{\pm}, f_0, w, g, h) \\ &= (X_0, \rho_0, \phi_0, k_0, \theta_0, \kappa_0, \mathbf{n}_0, v_0, f_{\pm 0}, f_{00}, w_0, g_0, h_0) \\ &+ \varepsilon (X_1, \rho_1, \phi_1, k_1, \theta_1, \kappa_1, \mathbf{n}_1, v_1, f_{\pm 1}, f_{01}, w_1, g_1, h_1), \end{aligned}$$

where ε is a parameter small in magnitude. Equations (2.5), (2.6), (4.1), and (4.2) imply

$$(4.31) \quad \theta_1 = -\partial_y X_1, \quad \kappa_1 = \partial_s \theta_1, \quad \mathbf{n}_1 = (0, \theta_1), \quad v_1 = \partial_t X_1,$$

$$(4.32) \quad k_\ell k_r = \frac{1}{4} ((k_\ell + k_r)^2 - (k_\ell - k_r)^2) = \frac{1}{4} (k^2 - \tan^2 \theta) = \frac{1}{4} k^2 + O(\varepsilon^2).$$

Now, inserting all the above expansions into (4.3)–(4.14), and using (4.17)–(4.25), (4.31), and (4.32), we obtain the following linearized system:

$$(4.33) \quad \nabla^2 \rho_1 = 0 \quad \text{for } |x - v_0 t| < L,$$

$$(4.34) \quad D_T \partial_x \rho_{1+} - F X_1 + f_{+1} = 0 \quad \text{at } x = v_0 t + L,$$

$$(4.35) \quad D_T \partial_x \rho_{1-} - F X_1 - f_{-1} = 0 \quad \text{at } x = v_0 t - L,$$

$$(4.36) \quad \partial_t \phi_1 - D_E \partial_y^2 \phi_1 = f_{+1} + f_{-1} - f_{01},$$

$$(4.37) \quad \partial_t k_1 - w_0 \partial_y^2 X_1 = 2(g_1 - h_1),$$

with the constitutive relations

$$(4.38) \quad f_{+1} = D_T \rho_{1+} - D_E \phi_1 - FLX_1,$$

$$(4.39) \quad f_{-1} = D_T \rho_{1-} - D_E \phi_1 + FLX_1,$$

$$(4.40) \quad f_{01} = -v_0 \phi_0 \partial_y^2 X_1 + \partial_t X_1,$$

$$(4.41) \quad w_1 = D_T(l_2 \rho_{1+} + l_3 \rho_{1-}) + l_1 D_E \phi_1 + (l_3 - l_2) FLX_1,$$

$$(4.42) \quad g_1 = D_T \phi_0 (m_2 \rho_{1+} + m_3 \rho_{1-}) + (m_1 D_E \phi_0 + g_0 / \phi_0) \phi_1 \\ + (m_3 - m_2) FL \phi_0 X_1,$$

$$(4.43) \quad h_1 = \frac{1}{4} D_T k_0^2 (n_2 \rho_{1+} + n_3 \rho_{1-}) + \frac{1}{4} n_1 D_E k_0^2 \phi_1 + \left(\frac{2h_0}{k_0} \right) k_1 \\ + \frac{1}{4} (n_3 - n_2) FL k_0^2 X_1,$$

$$(4.44) \quad \partial_t X_1 = w_0 k_1 + k_0 w_1,$$

where ρ_{1+} and ρ_{1-} denote the restriction of ρ_1 at $x = v_0 t + L$ and $x = v_0 t - L$, respectively.

The linearized system for the steady system (4.5)–(4.16) is the same, except that the two time derivative terms $\partial_t \phi_1$ and $\partial_t k_1$ are dropped from (4.36) and (4.37), respectively.

Dispersion relation. We seek solutions to the linearized system (4.33)–(4.44) of the form

$$(4.45) \quad \rho_1 = (\hat{r}_1 \cosh(lx) + \hat{s}_1 \sinh(lx)) e^{\omega t + i l y},$$

$$(4.46) \quad (X_1, \phi_1, k_1) = (\hat{X}_1, \hat{\phi}_1, \hat{k}_1) e^{\omega t + i l y},$$

where l is the wavenumber and \hat{r}_1 , \hat{s}_1 , \hat{X}_1 , $\hat{\phi}_1$, and \hat{k}_1 are constants. Here, ω is the growth rate, which depends on wavenumbers l . This dependence—the dispersion relation $\omega = \omega(l)$ —is determined by a cubic equation for the quasi-steady case and a linear equation for the steady case; cf. (C.1) and (C.2). So there are three growth rates ω (possible complex values) for the quasi-steady case. The dispersion relation for both cases is analyzed in Appendix C. In particular, its asymptotic behavior for large and small wavenumbers is described as follows.

Asymptotic analysis. Denote for each wavenumber $l \geq 0$ by $\omega = \omega(l)$ the growth rate (i.e., the root of the linear equation (C.2)) for the steady case and by $\omega_1 = \omega_1(l)$, $\omega_2 = \omega_2(l)$, and $\omega_3 = \omega_3(l)$ the growth rates (i.e., the three roots of the cubic equation (C.1)) for the quasi-steady case. Assume that $\omega_1(l)$ is always real and that $\omega_1(0) = 0$.

PROPOSITION 4.2. *For the steady system, we have*

$$(4.47) \quad \omega(l) = -v_0 \phi_0 l^2 + O(l^4) \quad \text{as } l \rightarrow 0,$$

$$(4.48) \quad \omega(l) = -\frac{v_0 w_0}{4h_0} l^2 + O(1) \quad \text{as } l \rightarrow \infty.$$

For the quasi-steady system, we have

$$(4.49) \quad \omega_1(l) = -v_0 \phi_0 l^2 + O(l^4) \quad \text{as } l \rightarrow 0,$$

and

$$(4.50) \quad \begin{aligned} \omega_1(l) &= -D_E l^2 + O(l), \\ \omega_2(l) &= R_0 + iw_0 l + O(l^{-1}), \\ \omega_3(l) &= R_0 - iw_0 l + O(l^{-1}), \end{aligned}$$

as $l \rightarrow \infty$, where $i = \sqrt{-1}$ and

$$(4.51) \quad R_0 = \frac{1}{4} D_E k_0 ((l_3 - l_2 - n_{23}) P_E - 2n_{123} \phi_0 - 2l_1 P_E \phi_0).$$

Moreover, $R_0 < 0$ for small edge Péclet number P_E . A sufficient condition for $R_0 < 0$ for all $P_E > 0$ is that

$$(4.52) \quad l_3 - l_2 - n_{23} \leq 0,$$

and a necessary condition for $R_0 < 0$ for all $P_E > 0$ is that

$$(4.53) \quad (l_3 - l_2 - n_{23}) l_{23}^2 m_{23} - 2l_1 n_{23} \leq 0.$$

The proof of these results is given in Appendix D.

5. Kinetic derivation of line tension and one-dimensional surface diffusion. As shown below, the kinetic edge model in the limit of small edge Péclet number yields a theory that is nearly as simple as the irreversible aggregation model. The asymptotic assumptions that underline this derivation are mathematically rather than physically based; i.e., they come from a “distinguished limit” rather than from a characterization of the size of the external sources that drive the problem.

5.1. Asymptotic expansion for small Péclet number. Consider the limiting adatom densities ρ_{\pm} , the fluxes f_{\pm} , and the curvature $\kappa = -X_{yy}$ to be parameters that are determined away from the boundary. Then the main equations are (4.3), (4.4), and (4.11) for ϕ , k , and v , respectively. In the scaling detailed below, the angle θ is of size $\varepsilon^{3/2}$ so that $\cos \theta \approx 1$; for simplicity, this approximation will be used from the beginning. Use the relations (4.5)–(4.10) to eliminate ρ_{\pm} , f_0 , w , g , and h , and write the resulting equations as

$$(5.1) \quad \begin{aligned} f_+ + f_- - v &= v\phi\kappa + \phi_t - D_E \phi_{yy}, \\ 2m_{123} D_E \phi^2 - \frac{1}{2} n_{123} D_E k^2 \phi &= -2\phi(m_2 f_+ + m_3 f_-) + \frac{1}{2} k^2 (n_2 f_+ + n_3 f_-) \end{aligned}$$

$$(5.2) \quad + k_t - \left(\left(\frac{v}{k} \right) X_y \right)_y,$$

$$(5.3) \quad v - l_{123} D_E \phi k = k(l_2 f_+ + l_3 f_-).$$

From the steady-state solution of section 3, the governing parameters in this system are $\varepsilon = P_E^{1/3}$, as defined in (4.26), and $\bar{f} = 2LF$. The steady-state solution from section 4 shows that

$$(k, \phi, v, f_{\pm}) = (\varepsilon k', \varepsilon^2 \phi', \bar{f} v', \bar{f} f'_{\pm}).$$

As shown below, the distinguished limit is

$$\begin{aligned} \kappa &= \varepsilon^2 \kappa', \\ Y &= \varepsilon^{-1/2} Y'. \end{aligned}$$

Since $\kappa = -X_{yy}$, this implies that $X = \varepsilon X'$ and also that $\theta = O(\varepsilon^{3/2})$ as stated earlier. In addition, the dispersion relation from Proposition 3.1 shows that the time scale is $T = \omega^{-1} = (-v\phi\ell^2)^{-1} = (-\bar{f}v'\varepsilon^2\phi'Y^{-2})^{-1} = O(\bar{f}^{-1}\varepsilon^{-3})$; i.e.,

$$T = \bar{f}^{-1}\varepsilon^{-3}T'.$$

Dividing (5.1) and (5.3) by \bar{f} , and dividing (5.2) by $D_E\varepsilon^4 = \bar{f}\varepsilon$, we obtain

$$\begin{aligned} f'_+ + f'_- - v' &= \varepsilon^4 v' \phi' \kappa' + \varepsilon^5 \phi'_{t'} - \phi'_{y'y'}, \\ 2m_{123}\phi'^2 - \frac{1}{2}n_{123}k'^2\phi' &= -2\varepsilon\phi'(m_2f'_+ + m_3f'_-) + \varepsilon\frac{1}{2}k'^2(n_2f'_+ + n_3f'_-) \\ &\quad + \varepsilon^3 k'_{t'} - \left(\left(\frac{v}{k}\right)X'_{y'}\right)_{y'}, \\ v' - l_{123}\phi'k' &= \varepsilon k'(l_2f'_+ + l_3f'_-). \end{aligned}$$

Notice that $\cos\theta = (1 + \tan^2\theta)^{-1/2} = (1 + X_y^2)^{-1/2} = 1 + O(\varepsilon^3)$. It follows that, to leading order (i.e., ignoring terms of size $O(\varepsilon)$), v' , k' , and ϕ' are given by

$$(5.4) \quad v' = f'_+ + f'_- + \phi'_{y'y'},$$

$$(5.5) \quad k' = (l_{123}\phi')^{-1}v',$$

$$(5.6) \quad 2m_{123}\phi'^2 - \frac{n_{123}}{2l_{123}^2}\phi'^{-1}v'^2 = -((l_{123}\phi')X'_{y'})_{y'}.$$

The result is more transparent if $X' = O(\delta)$ and $Y' = O(1/\delta)$ (i.e., $X = O(\delta\varepsilon)$ and $Y = O(\delta^{-1}\varepsilon^{-1/2})$), in which $\varepsilon \ll \delta \ll 1$, so that the previous equations (5.4)–(5.6) can be linearized, but additional terms of size $O(\varepsilon)$ from above are not required. Then ϕ' and v' are given by

$$(5.7) \quad \phi' = \left(\frac{n_{123}}{4m_{123}l_{123}^2}\right)^{1/3} (f'_+ + f'_-)^{2/3} - \frac{l_{123}}{6m_{123}}X'_{y'y'},$$

$$(5.8) \quad v' = f'_+ + f'_- + \phi'_{y'y'}.$$

5.2. Boundary conditions and velocity with line tension and one-dimensional surface diffusion. The boundary conditions for ρ from the kinetic edge model are (cf. (4.13)–(4.14), (4.5), and (4.6))

$$\begin{aligned} -D_T\mathbf{n} \cdot \nabla\rho_+ &= D_T\rho_+ - D_E\phi, \\ D_T\mathbf{n} \cdot \nabla\rho_- &= D_T\rho_- - D_E\phi. \end{aligned}$$

From these equations, we then obtain the new boundary conditions from (5.7) and the interface velocity from (5.8), after returning to the unprimed variables, as

$$(5.9) \quad -D_T\mathbf{n} \cdot \nabla\rho_+ = D_T(\rho_+ - \rho_*) - \mu\kappa,$$

$$(5.10) \quad D_T\mathbf{n} \cdot \nabla\rho_- = D_T(\rho_- - \rho_*) - \mu\kappa,$$

$$(5.11) \quad v = (f_+ + f_-) + \beta\rho_{*yy} + (\mu/D_E)\kappa_{yy},$$

where

$$\begin{aligned}\rho_* &= \left(\frac{n_{123}}{4m_{123}l_{123}^2} \right)^{1/3} \frac{D_E}{D_T} (f_+ + f_-)^{2/3}, \\ \mu &= \frac{l_{123}}{6m_{123}} D_E, \\ \beta &= \frac{D_T}{D_E}, \\ \kappa &= -X_{yy}.\end{aligned}$$

The boundary conditions (5.9) and (5.10) with a reference density ρ_* and a line tension term $\mu\kappa$ are of Gibbs–Thomson form, and the velocity formula (5.11) has the surface diffusion term $(\mu/D_E)\kappa_{yy}$. Note, however, the ρ_* is a steady-state value from [3], rather than the equilibrium value $\rho_{eq} = a^{-2}(D_K/D_T)$ in which D_K is the hopping rate from a kink [2,3]. The coefficient μ comes from a transition barrier energy and is unrelated to the thermodynamic value $\mu_{eq} = D_T^{-1}\rho_{eq}\Gamma$ [18] with $\Gamma = \gamma a^2/(k_B T)$ in which γ is step stiffness, k_B is Boltzmann’s constant, and T is temperature. The term $\beta\rho_{*yy}$ in the velocity formula (5.11) includes the effect of edge diffusion. To the best of our knowledge, this derivation, of Gibbs–Thomson form in the adatom boundary conditions and the surface diffusion term in the velocity, is the first that is based on microscopic (i.e., atomistic) dynamics, rather than thermodynamics.

6. The infinitely fast terrace diffusion limit. Assume that the adatoms diffuse infinitely fast and attach uniformly to step edges. Then the adatom density is $\rho = 0$ on steps, and the total flux to a step edge is

$$f = f_+ + f_- = 2FL.$$

Assume also that there is no detachment of atoms from an edge or a kink to a step. Then the original island dynamics model with step-edge kinetics is simplified to the following model—the simplified model of one-dimensional surface diffusion and kink convection with infinitely fast terrace diffusion limit

$$(6.1) \quad \partial_t \phi - D_E \partial_s^2 \phi = 2FL - v(\phi\kappa + 1),$$

$$(6.2) \quad \partial_t k - l_1 D_E \partial_s (\phi \partial_y X) = 2m_1 D_E \phi^2 - \frac{1}{2} n_1 D_E \phi k^2 + \frac{1}{2} n_1 D_E \phi (\partial_y X)^2,$$

$$(6.3) \quad v = l_1 D_E \phi k \cos \theta,$$

where D_E is the edge diffusion constant and the coefficients l_1 , m_1 , and n_1 are positive constants. This system involves only a moving step edge represented by the curve $x = X(y, t)$, the edge-atom density $\phi(y, t)$, and the kink density $k(y, t)$.

The steady-state solution for this system is given by

$$(6.4) \quad X_0(y, t) = v_0 t, \quad v_0 = 2FL, \quad \phi_0 = \frac{n_1}{4m_1} k_0^2, \quad k_0 = \left(\frac{4m_1}{l_1 n_1} P_E \right)^{1/3}.$$

The linearized system around this steady-state solution is given by

$$(6.5) \quad \partial_t \phi_1 - D_E \partial_y^2 \phi_1 + \partial_t X_1 - v_0 \phi_0 \partial_y^2 X_1 = 0,$$

$$(6.6) \quad \frac{1}{2} n_1 D_E k_0^2 \phi_1 - \partial_t k_1 - n_1 D_E \phi_0 k_0 k_1 + l_1 D_E \phi_0 \partial_y^2 X_1 = 0,$$

$$(6.7) \quad l_1 D_E k_0 \phi_1 + l_1 D_E \phi_0 k_1 - \partial_t X_1 = 0.$$

The existence of a nontrivial periodic solution (X_1, ϕ_1, k_1) of the form (4.46) leads to the dispersion relation $\omega = \omega(l)$ that is determined by

$$(6.8) \quad \begin{aligned} & (\omega/D_E)^3 + (l^2 + n_1 P_E/l_1 + l_1 k_0) (\omega/D_E)^2 \\ & + ((P_E n_1/l_1 + P_E^2 + l_1^2 \phi_0^2) l^2 + (3/2) n_1 P_E k_0) (\omega/D_E) \\ & + ((3n_1/2l_1) P_E^3 l^2 + l_1^2 \phi_0^2 l^4) = 0. \end{aligned}$$

If we drop the terms $\partial_t \phi$ and $\partial_t k$ in (6.1) and (6.2), respectively, we obtain the corresponding steady system

$$(6.9) \quad -D_E \partial_y^2 \phi = 2FL + v(\phi \partial_y \theta - 1),$$

$$(6.10) \quad -l_1 D_E \partial_y (\phi \partial_y X) = 2m_1 D_E \phi^2 - \frac{1}{2} n_1 d \phi k^2 + \frac{1}{2} n_1 D_E \phi (\partial_y X)^2,$$

$$(6.11) \quad v = l_1 D_E \phi k \cos \theta.$$

This system has the same steady-state solution as that for the unsteady system (6.1)–(6.3); cf. (6.4). The corresponding linearized system can be obtained by dropping the two terms $\partial_t \phi_1$ and $\partial_t k_1$ in (6.5)–(6.7). The dispersion relation in this case can be obtained explicitly as

$$(6.12) \quad \omega(l) = -\frac{l_1 D_E \phi_0 l^2 (2l_1 l^2 + 3n_1 P_E k_0^2)}{n_1 k_0 (2l^2 + 3l_1 k_0)}.$$

Notice that the dispersion relation for both the steady and unsteady systems of this model is of the form

$$\omega = D_E T(P_E, l)$$

with T a function of two variables.

Denote for each wavenumber $l \geq 0$ by $\omega_1 = \omega_1(l)$, $\omega_2 = \omega_2(l)$, and $\omega_3 = \omega_3(l)$ the three roots of the cubic equation (6.8). Assume that $\omega_1(l)$ is always real and that $\omega_1(0) = 0$. The following proposition gives the asymptotics of the dispersion relation for both small and large wavenumbers; its proof is similar to and much simpler than that for Proposition 4.2, and it is therefore omitted here.

PROPOSITION 6.1. *For the steady system, we have*

$$\omega(l) < 0 \quad \forall l > 0$$

and

$$\begin{aligned} \omega(l) &= -v_0 \phi_0 l^2 + O(l^4) & \text{as } l \rightarrow 0, \\ \omega(l) &= -\frac{v_0 w_0}{4h_0} l^2 + O(1) & \text{as } l \rightarrow \infty. \end{aligned}$$

For the unsteady system, we have

$$\begin{aligned} \omega_1(0) &= 0, & \operatorname{Re}(\omega_2(0)) &< 0, & \operatorname{Re}(\omega_3(0)) &< 0, \\ \omega_1(l) &= -v_0 \phi_0 l^2 + O(l^4) & \text{as } l \rightarrow 0, \end{aligned}$$

and

$$\begin{aligned} \omega_1(l) &= -D_E l^2 + O(1), \\ \omega_2(l) &= r_0 + iw_0 l + O(l^{-1}), \\ \omega_3(l) &= r_0 - iw_0 l + O(l^{-1}), \end{aligned}$$

as $l \rightarrow \infty$, where $i = \sqrt{-1}$ and

$$r_0 = -\frac{1}{2}D_E P_E \left(P_E + \frac{n_1}{l_1} \right) < 0.$$

By comparing Propositions 4.2 and 6.1, we see that the linear stability for both the original island dynamics model with step-edge kinetics and the simplified model with the infinitely fast terrace diffusion limit are similar. In particular, the dispersion relations for both of the corresponding steady systems are exactly the same in the limits of large and small wavenumber l . The origin of these similarities is that (C.1), which determines the growth rate ω for the edge kinetic model, does not contain the terrace diffusion constant D_T ; cf. the first five equations in Appendix C. This is due to the omission of the kinetic asymmetry and the use of the diffusion constant D_T as the attachment rate in the model.

7. Conclusions. We have rigorously analyzed four island dynamics models for step-flow growth. The irreversible aggregation model is linearly unstable, but the instability is weak. Since this model has the simplest boundary conditions, it can be used in combination with numerical stabilization techniques [5] for simulation of epitaxial growth. The edge kinetic model includes more physics, such as the edge diffusion and kink convection, and therefore is more complicated. But our analysis shows that it is linearly stable and that, in the large Péclet number limit, it leads to the Gibbs-Thompson term in the adatom boundary condition and the one-dimensional surface diffusion term in the step-edge velocity. These boundary conditions and velocity, together with the adatom diffusion equation, form an improved island dynamics model. Finally, a simplified model for the step-edge dynamics that does not involve the adatom density is derived from the kinetic edge model in the limit of infinitely fast terrace diffusion. The linear stability analysis of the new model confirms our analysis for the more complicated edge kinetic model.

Appendix A. Perturbation for free boundaries. In the analysis above, perturbation solutions are found for PDEs involving free boundaries. The method for this analysis is briefly described here. Consider a function

$$u = u(x, t, \varepsilon) = u_0 + \varepsilon u_1 + \dots$$

satisfying $u = 0$ at

$$x = X(t, \varepsilon) = X_0 + \varepsilon X_1 + \dots,$$

where ε is a parameter small in magnitude. This boundary condition is then

$$0 = u(X(t, \varepsilon), t, \varepsilon) = u_0(X_0(t), t) + \varepsilon (u_1(X_0(t), t) + X_1 \partial_x u_0(X_0(t), t)) + \dots.$$

It follows that the equations for u_0 and u_1 are

$$\begin{aligned} u_0(X_0(t), t) &= 0, \\ u_1(X_0(t), t) &= -X_1 \partial_x u_0(X_0(t), t). \end{aligned}$$

Appendix B. Proof of Proposition 4.1. Set for a fixed P_E (i.e., fixed $\varepsilon = P_E^{1/3}$)

$$H(\xi) = \xi(2m_{123}\xi + m_{23}\varepsilon^3)(2l_{123}\xi + l_{23}\varepsilon^3)^2 - \varepsilon^6(2n_{123}\xi + n_{23}\varepsilon^3) \quad \forall \xi \in \mathbf{R}.$$

It follows from (4.21)–(4.25) that

$$H(\phi_0) = 8D_E^{-3}w_0^2(g_0 - h_0) = 0.$$

However, one easily verifies that $H(0) < 0$, $H(\xi) \rightarrow +\infty$ as $\xi \rightarrow \infty$, and $H''(\xi) > 0$ for all $\xi \in \mathbf{R}$. Hence, ϕ_0 is the unique positive solution of $H(\xi) = 0$ for a fixed ε . Since ϕ_0 depends only on ε , we deduce from the steady-state solution (4.17)–(4.25) that k_0 , w_0/D_E , g_0/D_E , and h_0/D_E also depend only on ε . In particular, we have by (4.21) and (4.22) that

$$k_0 = 2\varepsilon^3(2l_{123}\phi_0 + l_{23}\varepsilon^3)^{-1}.$$

Direct calculations based on the fact that $H(\phi_0) = 0$ for each $\varepsilon > 0$ lead to the small ε asymptotics (4.27) and (4.28), and the following large ε asymptotics:

$$(B.1) \quad \phi_0 = \sigma_0 + \sigma_1\varepsilon^{-3} + O(\varepsilon^{-6}) \quad \text{as } \varepsilon \rightarrow \infty,$$

$$(B.2) \quad k_0 = \frac{2}{l_{23}} - \frac{4l_{123}\sigma_0}{l_{23}^2}\varepsilon^{-3} + O(\varepsilon^{-6}) \quad \text{as } \varepsilon \rightarrow \infty,$$

where σ_0 and σ_1 are defined in (4.29). Equations (B.1) and (B.2) imply (4.30).

Set $\xi = \phi_0$ as a function of ε . Differentiating both sides of the equation $H(\xi) = 0$ with respect to ε , we have by a series of calculations that

$$\frac{\varepsilon}{3\xi}\xi'(\varepsilon) = \frac{n_{23}\varepsilon^9 - l_{23}^2m_{23}\varepsilon^9\xi + 4l_{123}(2l_{23}m_{123} + l_{123}m_{23})\varepsilon^3\xi^3 + 16l_{123}^2m_{123}\xi^4}{n_{23}\varepsilon^9 + 2l_{23}(l_{23}m_{123} + 2l_{123}m_{23})\varepsilon^6\xi^2 + 8l_{123}(2l_{23}m_{123} + l_{123}m_{23})\varepsilon^3\xi^3 + 24l_{123}^2m_{123}\xi^4}.$$

Consequently, $\xi'(\varepsilon) > 0$ if $\xi \leq \sigma_0$. Moreover, if $\sigma_1 < 0$, then $\xi'(\varepsilon) > 0$ for large ε . Otherwise, if $\sigma_1 > 0$, then $\xi'(\varepsilon) < 0$ for large ε . These properties, together with (4.30), imply the rest of the proposition. \square

Appendix C. Dispersion relation. Inserting the expressions (4.38)–(4.43), (4.45), and (4.46) into (4.34)–(4.37) and (4.44), we get by a series of calculations that

$$\begin{aligned} D_T(l \cosh(lL) + \sinh(lL))\hat{s}_1 - F(1+L)\hat{X}_1 &= 0, \\ D_T(l \sinh(lL) + \cosh(lL))\hat{r}_1 - D_E\hat{\phi}_1 &= 0, \\ 2D_T \cosh(lL)\hat{r}_1 - (2D_E + D_E l^2 + \omega)\hat{\phi}_1 + (-v_0\phi_0 l^2 - \omega)\hat{X}_1 &= 0, \\ D_T G_r \cosh(lL)\hat{r}_1 + D_T G_s \sinh(lL)\hat{s}_1 + G_\phi\hat{\phi}_1 + (G_k - \omega)\hat{k}_1 + (G_X - w_0 l^2)\hat{X}_1 &= 0, \\ D_T V_r \cosh(lL)\hat{r}_1 + D_T V_s \sinh(lL)\hat{s}_1 + V_\phi\hat{\phi}_1 + V_k\hat{k}_1 + (V_X - \omega)\hat{X}_1 &= 0, \end{aligned}$$

where

$$\begin{aligned} G_r &= 2m_{23}\phi_0 - \frac{1}{2}n_{23}k_0^2, \\ G_s &= 2(m_2 - m_3)\phi_0 - \frac{1}{2}(n_2 - n_3)k_0^2, \\ G_\phi &= 2m_1 D_E \phi_0 + \frac{2g_0}{\phi_0} - \frac{1}{2}n_1 D_E k_0^2, \\ G_k &= -\frac{4h_0}{k_0}, \\ G_X &= 2(m_3 - m_2)FL\phi_0 - \frac{1}{2}(n_3 - n_2)k_0^2 FL, \end{aligned}$$

and

$$\begin{aligned}
V_r &= l_{23}k_0, \\
V_s &= (l_2 - l_3)k_0, \\
V_\phi &= l_1 D_E k_0, \\
V_k &= w_0, \\
V_X &= (l_3 - l_2)k_0 FL.
\end{aligned}$$

Thus, there is a nonzero solution $(X_1, \rho_1, \phi_1, k_1)$ of the given form if and only if the determinant of the coefficient matrix of the above linear system for $(\hat{r}_1, \hat{s}_1, \hat{\phi}_1, \hat{k}_1, \hat{X}_1)$ vanishes.

Notice that this determinant is zero if $l = 0$. Assume $l \neq 0$. After factoring $D_T \cosh(lL)$ and $D_T \sinh(lL)$ from the first and second columns of the determinant, respectively, the condition that the determinant is zero becomes

$$\text{(C.1)} \quad \begin{vmatrix} 0 & l \coth(lL) + 1 & 0 & 0 & -F(1+L) \\ l \tanh(lL) + 1 & 0 & -D_E & 0 & 0 \\ 2 & 0 & -(2D_E + D_E l^2 + \omega) & 0 & -v_0 \phi_0 l^2 - 1\omega \\ G_r & G_s & G_\phi & G_k - \omega & G_X - w_0 l^2 \\ V_r & V_s & V_\phi & V_k & V_X - \omega \end{vmatrix} = 0.$$

This determines the dispersion relation $\omega = \omega(l)$ for $l \neq 0$ for the quasi-steady system.

For the steady system, the dispersion relation $\omega = \omega(l)$ for $l \neq 0$ is determined similarly by

$$\text{(C.2)} \quad \begin{vmatrix} 0 & l \coth(lL) + 1 & 0 & 0 & -F(1+L) \\ l \tanh(lL) + 1 & 0 & -D_E & 0 & 0 \\ 2 & 0 & -(2D_E + D_E l^2) & 0 & -v_0 \phi_0 l^2 - \omega \\ G_r & G_s & G_\phi & G_k & G_X - w_0 l^2 \\ V_r & V_s & V_\phi & V_k & V_X - \omega \end{vmatrix} = 0.$$

A simple manipulation of the above determinants using the fact that all v_0/D_E , w_0/D_E , ϕ_0 , and k_0 depend only on the edge Péclet number P_E shows that these dispersion relations are of the form

$$\omega(l) = D_E S(L, P_E, l),$$

where S is a function of three variables. In particular, the dispersion relation is independent of the adatom hopping rate D_T for both the steady and quasi-steady systems. This results from the exclusion of the Ehrlich–Schwoebel effect [7, 21, 22] in our assumption.

Appendix D. Proof of Proposition 4.2. Consider first the steady system.

By (C.2) we have $\omega(l) = A(l)/B(l)$, where

$$A(l) = \begin{vmatrix} 0 & l \coth(lL) + 1 & 0 & 0 & -F(1+L) \\ l \tanh(lL) + 1 & 0 & -D_E & 0 & 0 \\ 2 & 0 & -(2D_E + D_E l^2) & 0 & -v_0 \phi_0 l^2 \\ G_r & G_s & G_\phi & G_k & G_X - w_0 l^2 \\ V_r & V_s & V_\phi & V_k & V_X \end{vmatrix},$$

$$B(l) = \begin{vmatrix} 0 & l \coth(lL) + 1 & 0 & 0 & 0 \\ l \tanh(lL) + 1 & 0 & -D_E & 0 & 0 \\ 2a & 0 & -(2D_E + D_E l^2) & 0 & 1 \\ G_r & G_s & G_\phi & G_k & 0 \\ V_r & V_s & V_\phi & V_k & 1 \end{vmatrix}.$$

By expanding $A(l)$ and $B(l)$ along the first row and the last column, respectively, we get that

$$A(l) = v_0 \phi_0 q_0 l^2 + O(l^4) \quad \text{and} \quad B(l) = -q_0 + O(l^2) \quad \text{as } l \rightarrow 0,$$

where

$$q_0 = \begin{vmatrix} 1 & -D_E & 0 \\ G_r & G_\phi & G_k \\ V_r & V_\phi & V_k \end{vmatrix} = 4l_{123} D_E h_0 + 2m_{123} D_E \phi_0 w_0 + \frac{1}{2\phi_0} n_{23} k_0^2 w_0 F L > 0,$$

and that

$$A(l) = D_E w_0^2 l^6 + O(l^4) \quad \text{and} \quad B(l) = D_E G_k l^4 + O(l^2) \quad \text{as } l \rightarrow \infty.$$

These imply (4.47) and (4.48).

Consider now the quasi-steady system. Notice first that $\omega_1(l) \rightarrow \omega_1(0) = 0$ as $l \rightarrow 0$. By a series of calculations, we get from (C.1) that

$$q_0 (\omega_1(l) + v_0 \phi_0 l^2) + O(l^4) + O(l^2 \omega_1(l)) + O(\omega_1(l)^2) = 0 \quad \text{as } l \rightarrow 0,$$

implying (4.49).

Observe from (C.1) that $|\omega(l)| \rightarrow \infty$ as $l \rightarrow \infty$. A simple manipulation of the determinant (C.1) leads to

$$\begin{vmatrix} -(2D_E + D_E l^2 + \omega) & 0 & -v_0 \phi_0 l^2 - \omega \\ G_\phi & G_k - \omega & G_X - w_0 l^2 \\ V_\phi & V_k & V_X - \omega \end{vmatrix} + O(l|\omega|) + O(|\omega|^2/l) = 0$$

for large l . Consequently,

$$\begin{aligned} \omega^3 + D_E l^2 \omega^2 + (2D_E + V_\phi - G_k - V_X) \omega^2 + (w_0^2 - D_E G_k - D_E V_X + V_\phi v_0 \phi_0) l^2 \omega \\ + D_E w_0^2 l^4 + O(l|\omega|) + O(|\omega|^2/l) + O(l^2) = 0 \quad \text{as } l \rightarrow \infty. \end{aligned} \tag{D.1}$$

It then follows immediately that there exist constants $c_1 > 0$ and $c_2 > 0$ such that

$$c_1 l \leq |\omega(l)| \leq c_2 l^2 \quad \text{for large } l.$$

If $|\omega(l)|/l^2$ is bounded below by a positive constant for large l , then (D.1) implies that

$$(D.2) \quad \omega(l) = -D_E l^2 + O(l) \quad \text{as } l \rightarrow \infty.$$

If, on the other hand, up to a subsequence of $\{l\}$, $\omega(l)/l^2 \rightarrow 0$ as $l \rightarrow \infty$, then we must have that $\omega(l) = O(l)$, for otherwise we would have a contradiction to (D.1). Therefore, the highest order terms in (D.1) are those of $l^2\omega^2$ and l^4 . Consequently, we have

$$(D.3) \quad \omega(l) = R(l) + i\sigma w_0 l \quad \text{as } l \rightarrow \infty,$$

where $R(l)$ is a bounded function of l and $\sigma = 1$ or -1 . If we plug the above expression back into (D.1), we then have

$$(D.4) \quad R(l) = R_0 + O(l^{-1}) \quad \text{as } l \rightarrow \infty,$$

where R_0 is defined by (4.51). Now, (4.50) follows from (D.2)–(D.4).

Finally, the fact that $R_0 < 0$ for small edge Péclet number P_E follows from (4.27) and (4.28). The condition (4.52) is obviously sufficient for $R_0 < 0$ for all P_E . The necessary condition (4.53) follows from (4.30). \square

REFERENCES

- [1] G. S. BALES AND A. ZANGWILL, *Morphological instability of a terrace edge during step-flow growth*, Phys. Rev. B, 41 (1990), pp. 5500–5508.
- [2] W. K. BURTON, N. CABRERA, AND F. C. FRANK, *The growth of crystals and the equilibrium of their surfaces*, Phil. Trans. Roy. Soc. London Ser. A, 243 (1951), pp. 299–358.
- [3] R. E. CAFLISCH, W. E. M. F. GYURE, B. MERRIMAN, AND C. RATSCH, *Kinetic model for a step edge in epitaxial growth*, Phys. Rev. E, 59 (1999), pp. 6879–6887.
- [4] R. E. CAFLISCH, M. F. GYURE, B. MERRIMAN, S. OSHER, C. RATSCH, D. VVEDENSKY, AND J. ZINK, *Island dynamics and the level set method for epitaxial growth*, Appl. Math. Lett., 12 (1999), pp. 13–22.
- [5] S. CHEN, M. KANG, B. MERRIMAN, R. E. CAFLISCH, C. RATSCH, R. FEDKIW, M. F. GYURE, AND S. OSHER, *Level set method for thin film epitaxial growth*, J. Comput. Phys., 167 (2001), pp. 475–500.
- [6] S. CLARKE AND D. VVEDENSKY, *Growth kinetics and step density in reflection high-energy electron diffraction during molecular-beam epitaxy*, J. Appl. Phys., 63 (1988), pp. 2272–2283.
- [7] G. EHRLICH AND F. G. HUDDA, *Atomic view of surface diffusion: Tungsten on tungsten*, J. Chem. Phys., 44 (1966), pp. 1039–1099.
- [8] R. GHEZ, H. G. COHEN, AND J. B. KELLER, *The stability of growing or evaporating crystals*, J. Appl. Phys., 73 (1993), pp. 3685–3693.
- [9] R. GHEZ AND S. S. IYER, *The kinetics of fast steps on crystal surfaces and its application to the molecular beam epitaxy of silicon*, IBM J. Res. Develop., 32 (1988), pp. 804–818.
- [10] M. F. GYURE, C. RATSCH, B. MERRIMAN, R. E. CAFLISCH, S. OSHER, J. ZINCK, AND D. VVEDENSKY, *Level set method for the simulation of epitaxial phenomena*, Phys. Rev. E, 58 (1998), pp. R6927–R6930.
- [11] A. KARMA AND C. MISBAH, *Competition between noise and determinism in step flow growth*, Phys. Rev. Lett., 71 (1993), pp. 3810–3813.
- [12] J. B. KELLER, H. G. COHEN, AND G. J. MERCHANT, *The stability of rapidly growing crystals*, J. Appl. Phys., 73 (1993), pp. 3694–3697.
- [13] F. LIU AND H. METIU, *Stability and kinetics of step motion on crystal surfaces*, Phys. Rev. E, 49 (1997), pp. 2601–2616.
- [14] B. MERRIMAN, R. E. CAFLISCH, AND S. OSHER, *Level set methods with applications to island dynamics*, in Free Boundary Problems: Theory and Applications, I. Athanasopoulos, G. Makrakis, and J. F. Rodrigues, eds., Chapman and Hall/CRC, Boca Raton, FL, 1999, pp. 51–70.
- [15] W. W. MULLINS AND R. F. SEKERKA, *Morphological stability of a particle growing by diffusion or heat flow*, J. Appl. Phys., 34 (1963), pp. 323–329.

- [16] W. W. MULLINS AND R. F. SEKERKA, *Stability of a planar interface during solidification of a dilute binary alloy*, J. Appl. Phys., 35 (1964), pp. 444–451.
- [17] O. PIERRE-LOUIS, *Continuum model for low temperature relaxation of crystal shapes*, Phys. Rev. Lett., 87 (2001), pp. 106104/1–4.
- [18] A. PIMPINELLI AND J. VILLAIN, *Physics of Crystal Growth*, Cambridge University Press, Cambridge, UK, 1998.
- [19] P. POLITI, G. GRENET, A. MARTY, A. PONCHET, AND J. VILLAIN, *Instabilities in crystal growth by atomic or molecular beams*, Phys. Rep., 324 (2000), pp. 271–404.
- [20] P. POLITI AND J. VILLAIN, *Ehrlich-Schwoebel instability in molecular-beam epitaxy: A minimal model*, Phys. Rev. B, 54 (1996), pp. 5114–5129.
- [21] R. L. SCHWOEBEL, *Step motion on crystal surfaces II*, J. Appl. Phys., 40 (1969), pp. 614–618.
- [22] R. L. SCHWOEBEL AND E. J. SHIPSEY, *Step motion on crystal surfaces*, J. Appl. Phys., 37 (1966), pp. 3682–3686.